The American Journal of Pathology, Vol. 172, No. 6, June 2008

DOI: 10.2353/ajpath.2008.070967

Immunopathology and Infectious Disease

Longitudinal *in Vivo* Positron Emission Tomography Imaging of Infected and Activated Brain Macrophages in a Macaque Model of Human Immunodeficiency Virus Encephalitis Correlates with Central and Peripheral Markers of Encephalitis and Areas of Synaptic Degeneration

Sriram Venneti,* Dafna Bonneh-Barkay,* Brian J. Lopresti,† Stephanie J. Bissel,* Guoji Wang,* Chester A. Mathis,† Michael Piatak, Jr.,‡ Jeffrey D. Lifson,‡ Julia O. Nyaundi,§ Michael Murphey-Corb,§ and Clayton A. Wiley*

From the Departments of Pathology, Radiology,† and Molecular Genetics and Biochemistry,§ University of Pittsburgh School of Medicine, Pittsburgh, Pennsylvania; and the Laboratory of Retroviral Pathogenesis,‡ AIDS Vaccine Program, Science Applications International Corporation Frederick, National Cancer Institute at Frederick, Frederick, Maryland*

Human immunodeficiency virus encephalitis is characterized by infiltration of the brain with infected and activated macrophages; however, it is not known why disease occurs after variable lengths of infection in 25% of immunosuppressed acquired immune deficiency syndrome patients. We determined *in vivo* correlates (in peripheral blood and the central nervous system) for the development and progression of lentiviral encephalitis by longitudinally following infected and activated macrophages in the brain using positron emission tomography (PET). Using human postmortem brain tissues from both lentivirus-infected encephalitic patients and cell culture systems, we showed that the PET ligand [^{3}H](R)-PK11195 bound specifically to virus-infected and activated macrophages. We longitudinally imaged infected and activated brain macrophages in a cohort of macaques infected with simian immunodeficiency virus using [^{11}C](R)-PK11195. [^{11}C](R)-PK11195 retention *in vivo* in the brain correlated with viral burden in the brain and cerebrospinal fluid, and with regions of both presynaptic and postsynaptic damage. Finally, longitudinal changes in [^{11}C](R)-PK11195 retention in the brain *in vivo* correlated with changes in circulating monocytes as well as in both natural killer and memory CD4^{+} T cells in the periphery. Our results suggest that development and progression of simian immunodeficiency virus encephalitis *in vivo* correlates with changes in specific cell subtypes in the periphery. A combination of PET imaging and the assessment of these peripheral immune parameters may facilitate longitudinal assessment of lentiviral encephalitis in living patients as well as evaluation of therapeutic efficacies. *(Am J Pathol 2008, 172:1603–1616; DOI: 10.2353/ajpath.2008.070967)*

Neurological deficits associated with human immunodeficiency virus (HIV) infection are seen in approximately one in four terminally immunosuppressed patients ranging from frank dementia (HIV-associated dementia, HIVD) to minor cognitive impairments.[1–3] In macaque models of acquired immune deficiency syndrome (AIDS) a variable percentage of infected animals also develop neurological disease.[4] The pathological diagnosis of neurological disease in humans and macaques is termed HIV and simian immunodeficiency virus (SIV) encephalitis (HIVE or SIVE), respectively (collectively referred to as lentiviral encephalitis), characterized by infiltration of the brain with abundant infected and ac-

Supported by the National Institutes of Health (RO1 MH071151 and K24 MH01717 to C.A.W.).

S.V. and D.B.-B. contributed equally to this study.

Accepted for publication February 21, 2008.

Address reprint requests to Dr. Clayton A. Wiley, Presbyterian University Hospital, Neuropathology Division, 200 Lothrop St. A515, Pittsburgh, PA 15213. E-mail: wiley1@pitt.edu.

tivated macrophages, multinucleated giant cells, and microglial nodules.[5,6]

Why a subset of lentiviral-infected hosts develops encephalitis and others do not is unknown. Both viral and host factors have been hypothesized to influence the development of lentiviral encephalitis. Virus isolated from the brains of both humans and macaques with encephalitis is macrophage-tropic suggesting that viral cell tropism is a key factor.[7,8] Further studies undertaken to isolate specific neurotropic strains of virus have not reached a consensus.[9,10]

The impact of host factors regulating systemic viral illness on the development of encephalitis is less understood. HIV-infected patients that show rapid and lethal progression with neurological symptoms show lower $CD4^+$ T-cell counts with greater abundance of macrophage infiltration in the central nervous system (CNS).[11,12] Similarly, rapid disease progression to AIDS in SIV-infected macaques is associated with the development of encephalitis.[13,14] These studies suggest that early collapse of peripheral viral control might contribute to development of encephalitis. The observation that HIVD may decrease in incidence and severity in patients with combination anti-retroviral therapies may be attributable to better peripheral viral control even though few antiretroviral drugs attain effective concentrations in the CNS.[15,16] Despite advances in anti-retroviral therapy, HIVD still remains a significant cause of morbidity, the determinants of which remain poorly understood, in part attributable to an inability to assess disease onset and progression in infected individuals while alive.

We have shown that [^{11}C](R)-PK11195, a ligand that binds specifically to the peripheral benzodiazepine receptor (PBR) enriched in activated brain macrophages,[17] is able to detect encephalitis in terminally ill macaques *in vivo* using positron emission tomography (PET).[18] We now show that PK11195 binds to infected macrophages and is able to detect the onset and progression of encephalitis *in vivo* when followed longitudinally using PET in SIV-infected macaques and correlates with areas of synaptic damage in brain tissues. Further, the development and progression of encephalitis correlates specifically with increases in cerebrospinal fluid (CSF) viral loads, peripheral elevated circulating monocyte and natural killer (NK) cell numbers and with decreases in circulating $CD4^+$ memory T cells, but not with changes in circulating total peripheral blood mononuclear cells (PBMCs), $CD4^+$ and $CD8^+$ T lymphocytes, activated subsets of monocytes, and platelet counts.

Materials and Methods

Animals

Animals were housed and maintained according to standards of the Association for Assessment and Accreditation of Laboratory Animal Care. The University of Pittsburgh Institutional Animal Care and Use Committee approved all experiments. Seven pigtailed macaques (*Macaca nemestrina*) varying from ages 74 to 93 months were challenged with SIVDeltaB670 viral swarm (SIVdB670) intravenously with the length of infection varying from 42 to 174 days and were sacrificed when moribund with AIDS.

Cell Culture

Macrophage cultures were prepared from human PBMCs (Central Blood Bank, Pittsburgh, PA).[19] Macrophages were activated with 1 μg/ml (concentration based on EC_{50}) of lipopolysaccharide (LPS) (*Escherichia coli* 0111/B4, from Sigma, St. Louis, MO)[20] or 300 international units (IU) of interferon (IFN)-γ (Sigma) for 48 hours, or infected with HIV-1 ADAM for 7 days confirmed by p24 levels in culture supernatants (data not shown). Primary human embryonic astrocytes were obtained from human fetal tissue collected as per standards of the University of Pittsburgh ethics and biosafety guidelines and cultured using established protocols.[21] Astrocytes were activated with 100 μmol/L dibutyryl cyclic AMP (dB-cAMP, Sigma)[22] or 1 μg/ml of LPS for 48 hours or were treated with HIV-1 ADAM for 7 days.

Filtration Radioligand Binding Assays

Filtration binding assays were performed as described previously.[18] Briefly, postmortem encephalitic brain tissue from the mid-frontal cortex of each case (Table 1) and whole cell preparations of macrophage and astrocyte cultures were homogenized in ice-cold 50 mmol/L HEPES buffer (pH 7.4). Total binding (per mg tissue) was determined by incubating homogenates (protein concentration, 50 to 200 μg) with 0.5 to 100 nmol/L [^{3}H](R)-PK11195 at 4°C for 2 hours in a final volume of 250 μl of HEPES. Nonspecific binding was determined by the inclusion of 10 μmol/L PK11195. Specific binding (fmol/mg protein) was defined as the difference between total and nonspecific binding. All samples were run in duplicate.

PET Imaging

PET imaging was conducted as previously described.[18] High specific activity [^{11}C](R)-PK11195 ([*N*-methyl-^{11}C]-PK11195) was synthesized at the University of Pittsburgh PET Facility as described.[23] At the end of 40 minutes synthesis specific activity was $\geq$2.0 Ci/μmol with chemical and radiochemical purities $\geq$95%. The yield of high purity [^{11}C](R)-PK11195 was in the range of 40 to 100 mCi. Macaques were imaged with [^{11}C](R)-PK11195 before infection (baseline) and at the indicated time points after infection (Table 2). Transmission scans were conducted using rotating ^{68}Ga/^{68}Ge rod sources after which $\sim$5 mCi (average dose, 4.92 $\pm$ 0.6 mCi; range, 3.33 to 5.92 mCi) of high specific activity [^{11}C](R)-PK11195 injected intravenously into each macaque. PET data were acquired in three-dimensional imaging mode using a microPET P4 scanner (Concorde Microsystems, Knox-

Table 1. Demographics of Cases Used to Obtain Human Frozen and Paraffin-Embedded Brain Tissues

Case no.	Age	Sex	Race	PMI (hours)	HIV infection	Neuropathological diagnosis	ART
1	36	M	C	23	Yes	HIVE	None
2	47	M	C	24	Yes	HIVE	None
3	28	M	AA	18	Yes	HIVE	None
4	31	M	C	21	Yes	HIVE	None
5	UN	M	UN	18	Yes	HIVE	UN
6	32	M	C	20	Yes	NPD	None
7	39	M	C	10	Yes	NPD	None
8	33	M	H	12	Yes	NPD	AZT, 1year
9	43	M	C	20	Yes	NPD	None
10	55	M	AA	25	Yes	NPD	None
11	60	M	C	<24	No	NPD	NA
12	69	M	C	<24	No	NPD	NA
13	54	F	C	<24	No	NPD	NA

PMI, post mortem interval; ART, antiretroviral therapy; M, male; F, female; C, Caucasian; AA, African American; H, Hispanic; UN, unknown; AZT, azidothymidine; NPD, no pathological diagnosis; NA, not applicable.

ville, TN), which simultaneously acquires 63 image planes (15.2-cm field of view) with a reconstructed image resolution of 5.8-mm full width, half maximum ramp filter. A dynamic series of PET scans was acquired for 90 minutes in 33 frames. Emission data were corrected for attenuation, dead time, scatter, and radioactive decay. [^{11}C](R)-PK11195 PET scans of each macaque were co-registered to the baseline PET scan using the automated image registration algorithm.[24] Regions of interest were defined on summed PET images (0 to 8 minutes after injection) and regional brain radioactivity concentrations summed over the scan frames were normalized to both the injected dose of [^{11}C](R)-PK11195 and the body mass of the animal (%ID/kg*g) to represent a semiquantitative measure of [^{11}C](R)-PK11195 binding to generate time-activity curves for the frontal cortex, basal ganglia, cerebellum, and brainstem. To compare longitudinal changes in [^{11}C](R)-PK11195 retention in each of these regions in each macaque, a measure of [^{11}C](R)-PK11195 retention was determined from each time activity curve by calculating the ratio between peak %ID/kg*g (~10 minutes) and baseline %ID/kg*g (70 minutes). [^{11}C](R)-PK11195 retention values thus calculated were validated by directly comparing these values with [^{3}H](R)-PK11195 binding values in brain tissues obtained from the same macaques in the same brain region. [^{11}C](R)-PK11195 PET retention *in vivo* correlated significantly with [^{3}H](R)-PK11195 maximal bound receptor (B_{max}) values suggesting that the [^{11}C](R)-PK11195 retention values *in vivo* closely mirrored the actual ligand binding values in brain tissues.

SIV RNA and DNA Quantification in Brain Tissues

Cell-associated SIV RNA and DNA were determined with modifications to the processing chemistry and protocols and assay conditions described in detail in Cline and colleagues.[25] Briefly, an approximate 10-mm^3 piece of frozen brain tissue from the frontal cortex was disrupted, in a closed tube, in 100 μl of proteinase K lysis solution using sonic energy supplied by a high-intensity cup horn and associated sonifier (Branson Ultrasonics Corporation, Danbury, CT). Typically, one to three cycles of sonication, each of 10-second duration at 60% power, were sufficient to completely disrupt the tissue and significantly reduce viscosity resulting from released chromatin. Total nucleic acids were then prepared as described, using proportionately twice the indicated volumes of reagents, and with the exception that 0.1% Tween 20 was included in the GuSCN secondary lysis solution to facilitate treatment of the larger amounts of membranous elements present. The resulting pellet containing RNA, DNA, and glycogen carrier was then suspended in 60 μl of 1× Turbo DNase buffer (Ambion, Inc., Austin, TX) and

Table 2. Macaque Experimental Parameters

Macaque no.	Species	Age at death (months)	Sex	Disease at time of sacrifice	Length of infection (days)	PET scan dates (days after infection)	Neuropathological diagnosis
CW06-280	Pigtailed	74	M	AIDS	174	0, 65, 100, 142, and 164	SIVE
CW06-282	Pigtailed	81	M	AIDS	42	0 and 42	SIVE
CW06-285	Pigtailed	93	M	AIDS	51	0 and 51	SIVE
CW06-286	Pigtailed	82	M	AIDS	51	0 and 51	SIVE
CW06-288	Pigtailed	83	M	AIDS	101	0, 51, 79, and 101	SIVE
CW06-289	Pigtailed	75	M	AIDS	128	0, 50, 99, and 120	SIV, no encephalitis
CW06-292	Pigtailed	81	M	AIDS	119	0, 50, and 106	SIV, no encephalitis

Seven pigtail macaques infected with SIV were imaged with three-dimensional PET using [^{11}C](R)-PK11195 longitudinally at the indicated time points in column 7. When macaques progressed to AIDS, they were sacrificed, after which they were grouped into SIVE or SIV infected, without encephalitis (SIV no E) categories based on the histopathology (frequency of distribution of multinucleated giant cells, microglial nodules, abundant activated and SIV-infected macrophages, perivascular chronic inflammation per ×10 and ×40 field in different brain regions).

divided into two equal aliquots. One aliquot was reserved for DNA testing; this aliquot was heated to 100°C for 5 minutes and then quenched on ice, before testing. The second aliquot for RNA testing was treated with 4 U of Turbo DNase for 30 minutes at 37°C and the RNA again extracted/recovered by addition of 120 μl of GuSCN solution, without additional Tween 20 or glycogen carrier, followed by alcohol precipitation. The DNA and RNA samples were tested separately. The copy numbers of SIV DNA (*gag*-specific target) and that of the gene sequence for macaque CCR5, as reference for cell equivalents, were co-determined in a duplex format quantitative reverse polymerase chain reaction (QPCR). The assay is as described, with omission of the reverse transcription step, and with the addition of primers (100 nmol/L final concentration each) and probe (100 nmol/L final concentration) specific for the macaque CCR5 sequence and use of a cloned genomic fragment of the Rhesus macaque CCR5 gene as standard (GenBank accession no. AF252567)[26] (plasmid pR1-D, of the *Macaca mulatta* CCR5 gene, promoter region was kindly provided by Dr. Sunil K. Ahuja, University of Texas, San Antonio, TX). Primer and probe sequences are as follows: forward primer (RHR5F01) 5′-CCAGAAGAGCTGCGACATCC-3′; reverse primer (RHR5R01) 5′-CTAATAGGCCAAGCAGCTGAGG-3′; probe (RHR5P01) 5′-(Texas Red) TTCCCCTACAAGAAACTCTCCCCGGTAAGTA (BHQ 2)-3′ (Biosearch Technologies, Novato, CA). Final reactions contained 1× PCR II buffer [50 mmol/L Tris-Cl, pH 8.3, 50 mmol/L KCl (Applied Biosystems, Foster City, CA)], 0.03% (w/v) gelatin, 0.012% (v/v) Tween 20, 4.5 mmol/L $MgCl_2$, 600 nmol/L each SIV gag primer, 100 nmol/L each macaque CCR5 primer, 100 nmol/L SIV gag probe (FAM label), 100 nmol/L CCR5 probe (Texas Red label), 50 nmol/L passive reference fluor, 5′-(Q670)TTTTTTTTTT(C3-blocked)-3′ (Biosearch Technologies), and 1.25 U of TaqGold polymerase (Applied Biosystems). The duplex QPCR assay was run on an MX3000P instrument (Stratagene, La Jolla, CA) using the following thermal profile: 95°C for 10 minutes to activate the TaqGold polymerase, followed by 45 cycles of 95°C for 30 seconds, 55°C for 15 seconds, and 60°C for 1 minute. Results are reported as nominal SIV gag DNA copy numbers per cell equivalents determined by copy numbers of CCR5 sequence, where there are four copies of CCR5 per cell (M.P., unpublished results). The cell-associated SIV gag RNA copy numbers were determined as described with these modifications: random hexamer primers were increased to 750 ng and reverse transcriptase was increased to 100 U to accommodate the relatively greater input of total RNA; concomitantly, the 85°C heat kill step in the reverse transcription thermal profile was extended to 30 minutes.

Quantification of SIV RNA in Plasma and CSF

One ml of plasma or 500 μl of CSF were centrifuged at 16,000 × *g* or 23,586 × *g* for1 hour, respectively, to pellet virions. Total RNA was extracted from the virus pellet using Trizol (Invitrogen, Carlsbad, CA). Real-time reverse transcriptase-polymerase chain reaction (PCR) was performed with 20 μl of each RNA sample as previously described using primers and probes specific for the SIV U5/LTR region.[27]

Immunohistochemistry

Immunostaining and laser confocal microscopic quantification was performed as described before.[18] Paraffin-embedded sections from the frontal cortex of macaques were stained with antibodies either to MAP-2 (Sternberger Monoclonals Inc., Lutherville, MD) or synaptophysin (SYN) (mouse monoclonal; DAKO, Carpinteria, CA) used at concentrations 1:1000 and 1:100, respectively, as described previously.[27] Sections were then incubated with Cy5-conjugated goat anti-mouse antibody at a concentration of 1:200 (Jackson ImmunoResearch Laboratories Inc., West Grove, PA). Immunostained sections were then scanned and quantified on a laser confocal microscope (LSM 150; Zeiss, Heidelberg, Germany) equipped with an argon laser with 458 nm, 477 nm, 488 nm, and 514 nm primary emission lines. Sections were scanned along the *z* axis to define the middle optical plane used in quantification (262,144 pixels/plane; 1 pixel = 0.25 μm^2). A Silicon Graphics computer (Windows NT 4.0 operating system; Microsoft, Redmond, WA) was used to perform image analysis using the LSM software (version 3.0, Zeiss). Scanning parameters such as laser power aperture, gain, and photomultiplier tube settings were kept constant for each wavelength.

An individual blinded to the experimental design imaged 10 areas (×40) encompassing 106,100 μm^2. Contributions to signal intensity from autofluorescence was minimized using a threshold that was kept constant. For each marker, the average pixel fluorescence and the pixel counts that exceeded the threshold were determined. The average pixel fluorescence multiplied by the total number of pixels was defined as the total florescence for a given marker. The total fluorescence values determined from the 10 scanned areas in one brain region were averaged to represent a measure of the cell phenotype in that brain region.

Combined Immunohistochemistry and Autoradiography

Frozen brain tissues were sectioned at 15 μm and mounted on Superfrost glass slides (Sigma). Sections were stained with antibodies against CD68 (1:50,000, mouse monoclonal; DAKO) and glial fibrillary acidic protein (GFAP) (1:500, rabbit polyclonal; DAKO) or HIV p24 (1:10, mouse monoclonal; DAKO). Sections were then incubated with Alexa Fluor 488-conjugated goat anti-mouse IgG and/or Cy3-conjugated goat anti-rabbit IgG (1:200, room temperature, 1 hour; Jackson ImmunoResearch Laboratories). Brain sections were then incubated with 1 nmol/L [^{3}H](R)-PK11195 for 30 minutes at 37°C and washed for 5 minutes at room temperature in 50 mmol/L HEPES buffer (pH 7.4) to determine total binding. Nonspecific binding was determined in adjacent brain sections in the presence of 1 μmol/L PK11195, respec-

tively. Slides were washed two times for 5 minutes each in buffer followed by distilled water, dried, and apposed to Kodak Bio-Max MR films (Eastman Kodak, Rochester, NY) for 3 weeks at room temperature, after which they were imaged on the confocal microscope.

Cell Counts

Peripheral blood samples were obtained from macaques at each PET imaging time point (Table 2). Complete and differential blood counts were obtained from each blood sample. Occasional time points were not available because of limited sample availability. PBMCs were isolated using ficoll-paque (Pharmacia Biotech, Piscataway, NJ) and counted as described previously.[28] Specific cell subtypes counts were obtained from peripheral blood samples using fluorochrome-conjugated monoclonal antibodies as previously detailed.[19,29] The following antibodies were used: anti-CD4 (BD Biosciences Pharmingen, San Diego, CA), anti-CD3 (Biosource, Camarillo, CA), anti-CD8 (DAKO), anti-CD29 (Beckman Coulter, Hialeah, FL), anti-CD14 (Beckman Coulter), and anti-CD16 (Beckman Coulter). Cell counts of $CD14^+$ (monocytes), $CD8^+/CD3^+$ ($CD8^+$ T cells), $CD4^+/CD3^+$ ($CD4^+$ T cells), $CD4^+/CD3^+/CD29^+$ (memory $CD4^+$ T cells), $CD14^+/CD16^+$ (activated subset of monocytes), and $CD3^-/CD16^+$ (NK cells) cells were determined on an XL2 flow cytometer (Beckman Coulter).

Western Blotting

Brain tissues from the frontal cortex of macaques with SIVE and SIV no E were homogenized with Lysis Buffer MT (Sigma) according to the manufacturer's protocol. Protein concentrations in each sample were determined by BCA protein assay (Pierce, Rockford, IL). Fifty μg of protein from each sample were separated out on a 12% sodium dodecyl sulfate-polyacrylamide gradient gel and were then transferred to Immun-Blot polyvinylidene difluoride membrane (Bio-Rad, Hercules, CA) by electrophoresis and blocked in 5% normal goat serum in Tris-buffered saline (TBS) (10 mmol/L Tris, pH 8.0, 150 mmol/L NaCl). Blots were washed three times in TBST (TBS 0.1% Tween 20) for 15 minutes. The membrane was incubated with a mouse monoclonal antibody against synaptophysin or MAP-2 (1:2000, or loading control-rabbit polyclonal to β-actin, 1:5000, after stripping the membrane; Abcam, Cambridge, MA). Membranes were then probed with goat anti-mouse or rabbit-horseradish peroxidase secondary antibodies (1:10,000; Jackson ImmunoResearch) The secondary antibody was washed extensively in TBS, three times for 20 minutes. The antibody was then visualized using enhanced chemiluminescence (Renaissance; NEN Life Science Products, Inc., Waltham, MA). Densitometric analysis was performed on a Macintosh computer using the public domain NIH Image program (developed at the National Institutes of Health and available on the Internet at *http://rsb.info.nih.gov/nih-image/*) v1.62.

Statistical Analysis

Data were analyzed using Prism software (Graphpad, San Diego, CA). Student's *t*-test or analysis of variance tests with posttest Bonferroni correction and 95% confidence intervals were used to analyze data. Nonparametric correlational analyses using 95% confidence intervals were performed to quantify the relationship between [^{11}C](R)-PK11195 retention and various parameters. Results from correlational analyses are represented by *r*, the Spearman's correlation coefficient.

Results

[^{3}H](R)-PK11195 Binding Is Higher in HIV Encephalitis and Corresponds to Activated and HIV-Infected Macrophages

Complete neuropathological microscopic analysis was performed in human brain tissues and no opportunistic infections were identified. Encephalitis was diagnosed on the basis of distribution of macrophage infiltrates, microglial nodules, multinucleated giant cells, and macrophages that immunostained for HIV p24 envelope protein in human brain tissues (Table 1).[5] Saturation filtration binding experiments using [^{3}H](R)-PK11195 were performed in postmortem tissues from the frontal cortex of patients with HIVE ($n = 5$), HIV infected, without encephalitis ($n = 5$), and noninfected controls ($n = 3$). The total number of binding sites (B_{max}) and ligand affinity (K_D) were compared in HIVE with HIV infected, without encephalitis, and noninfected controls. HIVE brain tissue showed a significant increase in [^{3}H](R)-PK11195 binding sites (B_{max}; Figure 1, A–C) ($P = 0.0006$) with no significant changes in K_D (Figure 1D) ($P = 0.488$) compared to both control groups.

In the resting CNS, PBR is expressed mainly on astrocytes and brain macrophages.[30] We wanted to determine the relative contributions of these two cell types to [^{3}H](R)-PK11195 binding in HIVE. We also wanted to evaluate the effects of viral infection and activation on [^{3}H](R)-PK11195 binding in macrophages. We determined changes in [^{3}H](R)-PK11195 binding on activation and infection in cultured primary human macrophages. Macrophage cultures were activated with 1 μg/ml of LPS or 300 IU of IFN-γ for 48 hours, or infected with HIV-1 for 7 days. [^{3}H](R)-PK11195 B_{max} (reflective of number of binding sites) was significantly higher in macrophages activated with either LPS or IFN-γ compared to untreated controls. Further, HIV (HIV-1 ADAM, a macrophage tropic viral strain)-infected macrophages showed significantly higher B_{max} compared to uninfected controls and macrophages activated with either LPS or IFN-γ (Figure 1E). Macrophages activated with either LPS or IFN-γ did not show changes in K_D compared to untreated controls. Macrophages infected with HIV showed an increase in K_D compared to uninfected controls (Figure 1F). Neither B_{max} nor K_D differed in primary human embryonic astrocytes treated with 100 μmol/L dB-

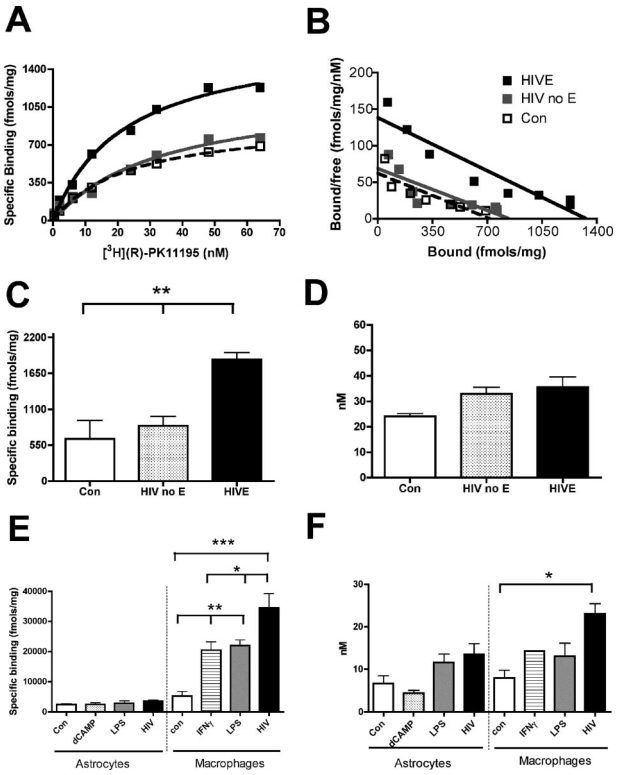

Figure 1. [^{3}H](R)-PK11195-specific binding is higher in HIVE brain tissues compared to controls and corresponds to HIV-infected and activated macrophages. **A** and **B:** Representative saturation binding curves (**A**) and Scatchard plots (**B**; X-intercept represents B_{max}, and slope represents K_D) with [^{3}H](R)-PK11195 from the mid-frontal cortex of human patients with HIVE (**black squares**), HIV no-encephalitis (**gray squares**), and age-matched controls (**clear squares**). **C:** B_{max} (fmol/mg protein, *y* axis), reflective of the total number of [^{3}H](R)-PK11195 binding sites/mg protein in HIVE ($n = 5$, **black bars**) compared to noninfected controls (Con, $n = 3$; **clear bars**) and HIV infected, without encephalitis (HIV no E, $n = 5$; **hatched bars**) frontal cortical brain tissue ($P = 0.0006$). **D:** [^{3}H](R)-PK11195 binding affinity (K_D, nmol/L, *y* axis) in HIVE ($n = 5$, **black bars**) compared to noninfected controls (Con, $n = 3$; **clear bars**) and HIV infected, without encephalitis (HIV no E, $n = 5$; **hatched bars**) frontal cortical brain tissue ($P = 0.2296$). **E:** [^{3}H](R)-PK11195 B_{max} (fmol/mg protein, *y* axis) in primary human astrocytes activated with 100 μmol/L dB-cAMP, treated with 1 μg/ml of LPS for 48 hours, or treated with HIV for 7 days compared to untreated controls ($n = 3$, each condition). B_{max} was also measured in primary human macrophages activated with either 1 μg/ml of LPS or 300 IU of IFN-γ for 48 hours and infected with HIV for 7 days compared to untreated controls ($n = 3$, each condition). **F:** [^{3}H](R)-PK11195 K_D (nmol/L protein, *y* axis) in primary human embryonic astrocytes activated with 100 μmol/L dB-cAMP, treated with 1 μg/ml of LPS for 48 hours, or treated with HIV for 7 days compared to untreated controls. K_D values in primary human macrophages activated with either 1 μg/ml of LPS or 300 IU of IFN-γ for 48 hours or infected with HIV for 7 days compared to untreated controls. All data were analyzed using one-sided analysis of variance, $^{***}P < 0.0001$, $^{**}P < 0.001$, and $^{*}P < 0.01$.

cAMP (dB-cAMP has been extensively used to model activation of astrocytes in culture[22]) or 1 μg/ml of LPS for 48 hours or with HIV for 7 days compared to untreated controls (Figure 1, E and F). These results were confirmed in postmortem tissues as autoradiography showed increased [^{3}H](R)-PK11195 binding in HIVE (Figure 2, E and H) compared with HIV infected, without encephalitis (Figure 2J). Further, [^{3}H](R)-PK11195 binding overlapped with CD68-labeled activated macrophages (Figure 2, C and F) and HIV p24-labeled infected macrophages (Figure 2, G and I) but not GFAP-labeled astrocytes (Figure 2, D and F).

Longitudinal [^{11}C](R)-PK11195 PET Imaging Differentiates Macaques that Developed Encephalitis from Macaques that Did Not

We imaged a group of seven pigtail macaques infected with SIVdB670 with [^{11}C](R)-PK11195 before infection and longitudinally after infection at various time points as indicated in Table 2. Macaques were sacrificed when they developed terminal AIDS with three animals rapidly progressing to AIDS (Table 2). Five of the seven SIV-infected macaques demonstrated increased uptake and retention of [^{11}C](R)-PK11195 with PET at the indicated time points after infection compared to baseline scans before infection in the frontal cortex (representative time activity curve Figure 3A), striatum (Figure 3C), cerebellum (Figure 3D), and brainstem (Figure 3E). Two macaques did not show increases in [^{11}C](R)-PK11195 retention from baseline in all of the assessed brain regions (Figure 3).

PET findings were compared with neuropathological features evaluated in all macaques at necropsy. SIVE was defined by the presence of parenchymal and perivascular macrophages, multinucleated giant cells, microglial nodules, and abundant macrophages that stained for the SIV envelope protein SIV gp110 (Figure 2). All five macaques that demonstrated increased [^{11}C](R)-PK11195 PET retention in the brain showed SIVE (Table 2). The remaining two macaques did not show any significant PET retention of [^{11}C](R)-PK11195 in the brain compared to baseline scans before infection (Figure 3). These animals failed to show any significant histopathological abnormalities and were therefore considered non-encephalitic SIV-infected controls. After PET scans macaques were sacrificed after which brain tissue was subjected to filtration binding assays with [^{3}H](R)-PK11195. [^{3}H](R)-PK11195 B_{max} values, reflective of the number of PK11195 binding sites, obtained from the frontal cortex (fmol/mg protein) in both SIVE and SIV-infected macaques without encephalitis were compared with [^{11}C](R)-PK11195 retention in the frontal cortex of the same macaques. [^{11}C](R)-PK11195 PET retention *in vivo* correlated significantly with [^{3}H](R)-PK11195 B_{max} values suggesting that the [^{11}C](R)-PK11195 retention values *in vivo* closely mirrored actual ligand binding values in brain tissues (Figure 3B).

Longitudinal [^{11}C](R)-PK11195 PET Retention in the Brain in Infected Macaques Correlates with CSF but Not with Plasma Viral Loads

We determined if longitudinal assessment of [^{11}C](R)-PK11195 retention in the CNS correlates with CSF viral loads in SIV-infected macaques. Viral copies per ml of CSF (Figure 4A) and plasma (Figure 4B) were determined at the same time points when macaques were imaged with [^{11}C](R)-PK11195 (Table 2). [^{11}C](R)-PK11195 retention in the frontal cortex at various time points correlated significantly with CSF viral loads ($r = 0.8274$, $P = 0.0003$) (Figure 4C), but not with plasma viral

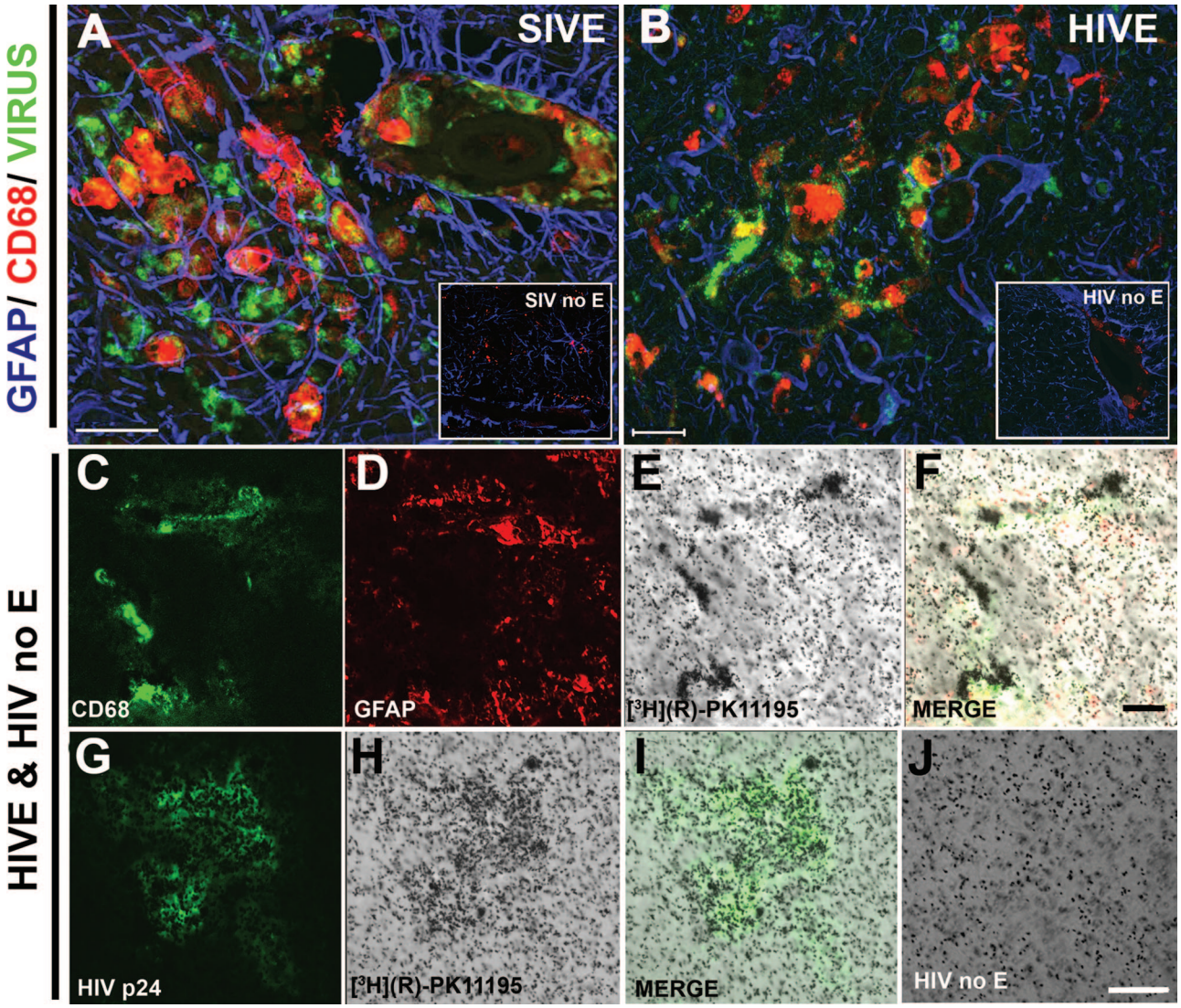

Figure 2. [^{3}H](R)-PK1195 binding corresponds to activated and infected macrophages in HIVE. **A** and **B:** Frontal cortical tissue obtained from macaques with SIVE (**A**) and SIV infected without encephalitis (SIV no E; **inset** in **A**) and patients with HIVE (**B**) and HIV infected without encephalitis (HIV no E; **inset** in **B**) were stained for reactive astrocytes (GFAP, blue), activated macrophages (CD68, red), and virus (green; **A**, SIV gp110; **B**, HIV p24). [^{3}H](R)-PK11195 autoradiography was performed in HIVE (**E** and **H**) and compared to HIV infected without encephalitis (HIV no; **E** and **J**). [^{3}H](R)-PK11195 autoradiography in HIVE brain tissues was combined with immunostaining for activated macrophages (**C**; CD68, green), astrocytes (**D**, GFAP, red; **F**, merge) and HIV-infected macrophages (**G**, HIV p24; **I**, merge). Scale bars: 50 μm (**A**); 20 μm (**B**, **F**); 100 μm (**J**).

loads (r = 0.1476, P = 0.5589) (Figure 4D). Similar results were obtained when longitudinal [^{11}C](R)-PK11195 retention data from the striatum, cerebellum, and brainstem were correlated with CSF and plasma viral loads (Table 3). These results suggest that changes in [^{11}C](R)-PK11195 retention in encephalitic macaques closely parallel changes in CSF, but not plasma, viral loads. Similar results were observed on comparing CSF and plasma viral loads with [^{3}H](R)-PK11195-binding values in brain tissues (Table 4).

Terminal PET [^{11}C](R)-PK11195 Retention in Vivo *Correlates with Postmortem Brain Viral Loads*

Viral RNA and DNA were determined in postmortem frontal cortical tissue of all macaques (left y axis, Figure 5A). Viral RNA and DNA were compared to terminal, premortem [^{11}C](R)-PK11195 retention values in the frontal cortex in these same animals (right y axis, Figure 5A). [^{11}C](R)-PK11195 retention correlated significantly with both SIV RNA (r = 0.9820, P = 0.0004) and DNA (r = 0.8487, P = 0.0238) (Figure 5B).

[^{11}C](R)-PK11195 Retention in Vivo *Correlates with Areas of Synaptic Degeneration*

To assess synaptic damage we immunostained frontal cortical tissue from all macaques with synaptophysin (SYN), a protein associated with neuronal presynaptic vesicles, and a postsynaptic protein, microtubule-associated protein-2 (MAP-2) present in neuronal cell bodies and dendrites. Decreases in SYN and MAP-2 have been

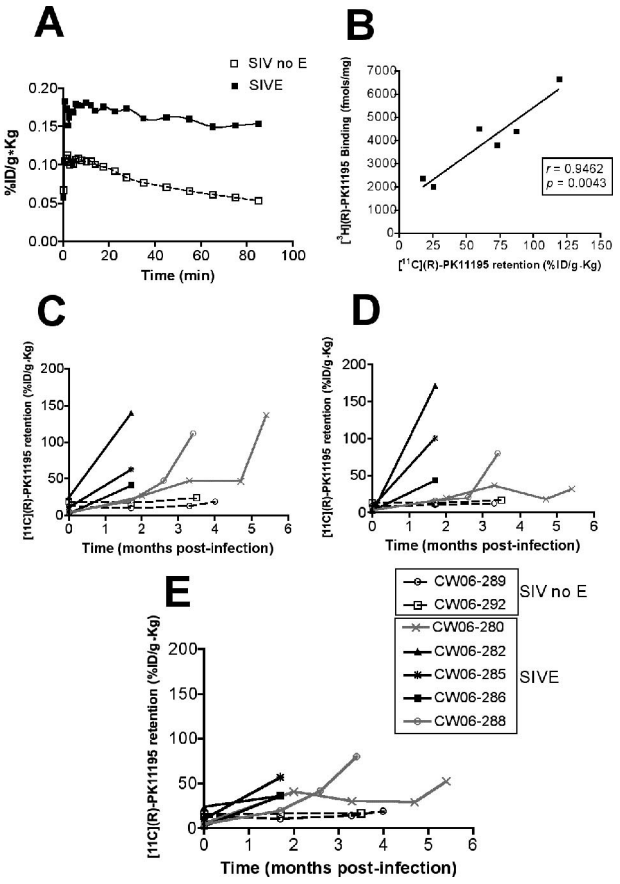

Figure 3. Longitudinal PET imaging *in vivo* shows higher retention of [^{11}C](R)-PK11195 in the brain in macaques that develop SIVE compared to SIV-infected macaques that do not develop encephalitis. Macaques infected with SIVdB670 were scanned with [^{11}C](R)-PK11195 longitudinally as indicated in Table 2 and were classified, retrospectively, into encephalitic (SIVE) and SIV infected, without encephalitis (SIV no E) groups, based on histopathology at necropsy. **A:** Representative time activity curves of [^{11}C](R)-PK11195 retention in the frontal cortex of macaques imaged before necropsy. [^{11}C](R)-PK11195 retention in the brain is represented as radioactivity concentrations summed over the scan frames and normalized to both the injected dose of [^{11}C](R)-PK11195 and the body mass of the animal (%ID/g*kg, *y* axis) and is plotted against time in minutes (*x* axis) in SIV encephalitic (SIVE, **black squares**) and SIV-infected macaques without encephalitis (SIV no E, **open squares**). **B:** [^{11}C](R)-PK11195 retention values (%ID/g*kg, *x* axis) in SIV-infected macaques from the frontal cortex was correlated with [^{3}H](R)-PK11195 B_{max} values (fmol/mg) in frontal cortical brain tissues obtained from the same macaques. **C–E:** Longitudinal PET imaging *in vivo* with [^{11}C](R)-PK11195 (%ID/g*kg, determined from time activity curves in each macaque in each brain region) at indicated time points after infection in SIVE macaques in the basal ganglia (**C**), cerebellum (**D**), and the brainstem (**E**).

reported in both HIVE and SIVE and have been used as markers for synaptic damage.[27,31] Both markers were decreased in SIVE macaques compared to nonencephalitic macaques (MAP-2, $P = 0.024$; and SYN, $P = 0.0002$) by immunofluorescence (Figure 6, A–C) and Western blotting (Figure 6D). [^{11}C](R)-PK11195 retention in the frontal cortex in these same animals correlated significantly with decreases in both SYN ($r = -0.9286$, $P = 0.0067$; Figure 6E) and MAP-2 ($r = -0.8929$, $P = 0.0123$; Figure 6F). [^{11}C](R)-PK11195 retention *in vivo* also correlated significantly with decreases in SYN ($r = -0.8617$, $P = 0.0127$; Figure 6G) and MAP-2 ($r = -0.8032$, $P = 0.0296$; Figure 6H) levels determined by Western blotting, which closely paralleled the immunofluorescence quantification data.

Longitudinal [^{11}C](R)-PK11195 PET Imaging in Infected Macaques Correlates with Changes in Circulating Peripheral Monocytes, NK Cells, and Memory CD4$^+$ T Cells

To determine correlates of encephalitis in the peripheral immune system *in vivo*, we longitudinally followed various immunological parameters that influence peripheral viral control in parallel with [^{11}C](R)-PK11195 PET imaging at the same time points in the same macaques. Total cell counts of various parameters were correlated with [^{11}C](R)-PK11195 retention in the midfrontal cortex (Figure 7A) longitudinally at the indicated time points (Table 2) during infection. Peripheral immunological parameters were determined using flow cytometry as cell counts of: PBMCs, CD3$^+$/CD4$^+$ T lymphocytes, CD3$^+$/CD8$^+$ T cells, CD14$^+$ monocytes (Figure 7B), CD14$^+$CD16$^+$ activated subsets of monocytes, CD3$^+$/CD4$^+$/CD29$^+$ memory subsets of CD4$^+$ T lymphocytes (Figure 7C), CD3$^-$/CD16$^+$ NK cells (Figure 7D) and platelets.

Of these various factors, significant positive correlation between [^{11}C](R)-PK11195 retention *in vivo* was found with numbers of peripheral circulating CD14$^+$ monocytes ($r = 0.8491$, $P < 0.0001$; Figure 7E). [^{11}C](R)-PK11195 retention *in vivo* in the midfrontal cortex correlated negatively with CD3$^+$/CD4$^+$/CD29$^+$ memory subsets of CD4$^+$ T lymphocytes ($r = -0.8396$, $P < 0.0001$; Figure 7F). Significant positive correlation was also found with CD3$^-$/CD16$^+$ NK cells ($r = 0.4993$, $P = 0.0295$; Figure 7G). None of the other cell types correlated with longitudinal [^{11}C](R)-PK11195 retention *in vivo* in the frontal cortex (Table 3). Similar data obtained from the striatum, cerebellum, and brainstem are summarized in Table 3. These results were confirmed in brain tissues using [^{3}H](R)-PK11195 (Table 4).

Discussion

We show that PK11195 labels infected and activated brain macrophages and can be used to detect the onset and progression of encephalitis *in vivo* using PET. Longitudinal increases in [^{11}C](R)-PK11195 retention in the brain *in vivo* correlated significantly with increases in CSF viral loads, total circulating monocytes, and NK cell numbers, and decreases in memory CD4$^+$ subsets of T lymphocytes but not with changes in CD4$^+$ and CD8$^+$ T lymphocytes, PBMCs, CD14$^+$/CD16$^+$ subsets of monocytes, and platelets. These data suggest that PET imaging with [^{11}C](R)-PK11195 and assessment of these peripheral immune parameters might help in the clinical detection and therapeutic monitoring of HIVD.

[^{3}H](R)-PK11195 binding was higher in HIVE brain tissues compared to HIV-infected patients without encephalitis and uninfected controls (Figure 1). In both cell culture and human postmortem tissues [^{3}H](R)-PK11195 binding corresponded to activated macrophages (Fig-

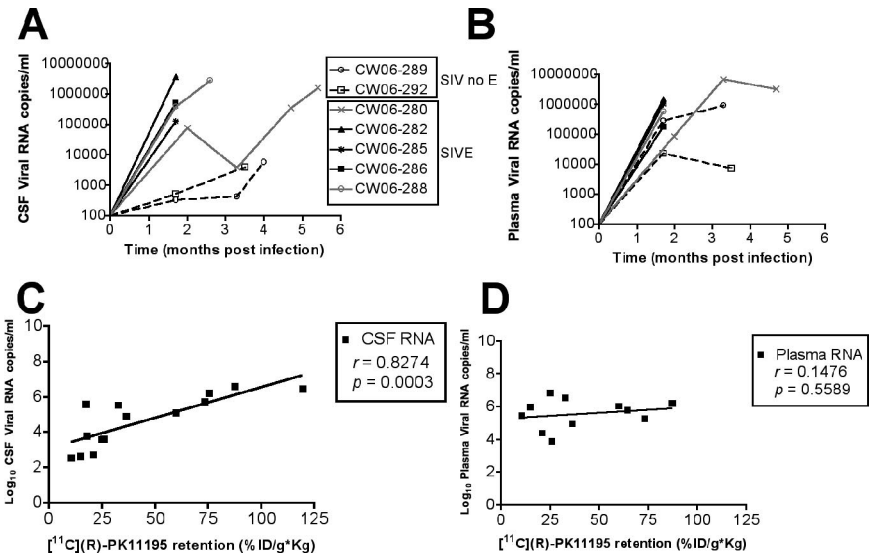

Figure 4. [^{11}C](R)-PK11195 retention in the brain *in vivo* during infection correlates with CSF viral loads. **A** and **B:** CSF (**A**, RNA copies/ml, *y* axis) and plasma viral loads (**B**, RNA copies/ml, *y* axis) were measured at the indicated times (months, *x* axis) in all infected macaques. **C** and **D:** Longitudinal retention of [^{11}C](R)-PK11195 in the frontal cortex (%ID/g*kg, *x* axis) at various time points after infection was correlated with CSF (**C**) and plasma viral loads (**D**, both Log_{10} RNA copies/ml, *y* axis).

ures 1 and 2). It is possible that the archival nature of human tissues influences the quality of the binding curves, despite this limitation, we observed increased PK11195 binding in lentiviral encephalitis compared to controls in brain tissues as well as in macaques *in vivo*. These data are in agreement with previous studies that have shown that PK11195 labels activated brain macrophages in SIVE.[18,32] However, the effects of viral infection on [^{3}H](R)-PK11195 binding are not known. [^{3}H](R)-PK11195 binding in HIV-infected macrophages was higher compared to uninfected controls and corresponded to HIV-infected macrophages in brain tissues (Figures 1 and 2). Moreover, terminal premortem values of [^{11}C](R)-PK11195 correlated significantly with both SIV RNA and DNA copies, suggesting that [^{11}C](R)-PK11195 labels infected brain macrophages. Further, K_D values in infected macrophages were higher compared to controls suggesting that the ligand-binding site may be altered in infected macrophages (Figure 1F), however, no changes in K_D values were observed in HIVE tissues compared to controls. PBR is thought to be a part of the mitochondrial permeability transition pore and influences cell death mechanisms by directly interacting with proteins regulating apoptosis.[33] Increased PBR expression is thought to protect cells from apoptotic insults.[34,35] Macrophages in culture when infected with HIV are able to survive for as long as 60 days.[36] It is possible that increased PK11195 binding in these cells, reflective of PBR expression, may play a role in increasing the life span of these cells. Further, increased PBR is also thought to alter the pore structure that may result in an alteration in K_D values in HIV-infected cells. Although an increase in K_D values were observed in HIV-infected cells *in vitro*, no differences in K_D values were observed in brain tissues in encephalitis versus control conditions mitigating against the possibility of changes in *in vivo* PET analyses. Future experiments examining the role of PBR in cell survival and HIV infection will address these questions.

The increase in PK11195 binding in lentiviral encephalitis may represent increases in both numbers of brain macrophages as well as increases in the total number of

Table 3. Relationship between Longitudinal [^{11}C](R)-PK11195 Retention in the Brain *in Vivo* with CSF and Other Peripheral Immunological Parameters during Infection

Brain region	Statistical parameter	CSF viremia	Plasma viremia	$CD14^+$	PBMC	$CD14^+/CD16^+$	$CD3^-/CD16^+$	$CD3^+/CD4^+$	$CD3^+/CD4^+/CD29^+$	$CD3^+/CD8^+$	Platelets
Cortex	*r*	0.8274	0.1476	0.8491	0.2127	0.3342	0.4993	−0.3386	−0.8396	−0.2097	−0.3
	P	0.0003	0.5589	<0.0001	0.3968	0.162	0.0295	0.1562	<0.0001	0.3888	0.2121
Striatum	*r*	0.6853	0.5636	0.6176	0.1361	0.3157	0.4688	−0.1517	−0.8419	−0.0867	−0.2405
	P	0.0139	0.071	0.0082	0.6024	0.2018	0.0497	0.5479	<0.0001	0.7322	0.3365
Cerebellum	*r*	0.7203	0.3818	0.517	0.04415	0.2669	0.4905	−0.2328	−0.8626	−0.087	−0.3015
	P	0.0082	0.2466	0.0336	0.871	0.3004	0.0456	0.3685	<0.0001	0.7397	0.2396
Brainstem	*r*	0.7005	0.2597	0.652	0.1725	0.3784	0.5294	−0.1703	−0.8417	−0.173	−0.2062
	P	0.0112	0.4406	0.0025	0.4936	0.1102	0.0198	0.4859	<0.0001	0.4789	0.397

Longitudinal [^{11}C](R)-PK11195 retention *in vivo* during infection in the indicated brain regions was correlated in the same macaques at the same time points with longitudinal changes in CSF (Figure 3A) and plasma viral loads (Figure 3B), and total peripheral blood cell counts (determined by flow cytometry) of $CD14^+$ monocytes (Figure 6B), peripheral blood mononuclear cells (PBMCs), $CD14^+/CD16^+$ activated subsets of monocytes, $CD3^-/CD16^+$ NK cells (Figure 6D), $CD3^+/CD4^+$ T lymphocytes, $CD3^+/CD4^+/CD29^+$ memory subsets of $CD4^+$ T lymphocytes (Figure 6C), $CD3^+/CD8^+$ T lymphocytes and platelets. Significant positive correlations between [^{11}C](R)-PK11195 retention *in vivo* in all assessed brain regions were found with CSF viral loads, numbers of peripheral $CD14^+$ monocytes, and $CD3^-/CD16^+$ NK cells. [^{11}C](R)-PK11195 retention *in vivo* correlated negatively with $CD3^+/CD4^+/CD29^+$ memory subsets of $CD4^+$ T lymphocytes. None of the other cell types correlated with longitudinal [^{11}C](R)-PK11195 retention *in vivo*. Correlations were performed using 95% confidence intervals. Results from correlational analyses are represented by *r*, the Spearman's coefficient and *P* values below 0.05 were considered significant.

Table 4. Relationship between [^{3}H](R)-PK11195 Binding in the Frontal Cortex with CSF, Synaptic Proteins, and Other Peripheral Immunological Parameters during Infection

Parameter	*r* value	*P* value
CSF viremia	0.8781	0.0501
Plasma viremia	0.4706	0.3463
SIV RNA	0.8179	0.0389
SIV DNA	0.8216	0.0449
$CD14^+$	0.8625	0.0271
PBMC	−0.01974	0.3594
$CD14^+/CD16^+$	0.9117	0.0114
$CD3^-/CD16^+$	0.9139	0.0108
$CD3^+/CD4^+$	0.4593	0.3594
$CD3^+/CD4^+/CD29^+$	−0.876	0.0500
$CD3^+/CD8^+$	−0.6295	0.1804
Platelets	0.3166	0.6037
MAP-2	−0.8674	0.0252
SYN	−0.866	0.0257

[^{3}H](R)-PK11195 B_{max} values from the mid frontal cortex were correlated with changes in terminal: 1) CSF and plasma viral loads; 2) total peripheral blood cell counts of $CD14^+$ monocytes, peripheral blood mononuclear cells (PBMCs), $CD14^+/CD16^+$ activated subsets of monocytes, $CD3^-/CD16^+$ NK T cells, $CD3^+/CD4^+$ T lymphocytes, $CD3^+/CD4^+/CD29^+$ memory subsets of $CD4^+$ T lymphocytes, $CD3^+/CD8^+$ T lymphocytes and platelets; and 3) the presynaptic marker SYN and postsynaptic marker MAP-2. Significant positive correlations were observed between [^{3}H](R)-PK11195 B_{max} values with CSF viral loads, numbers of peripheral $CD14^+$ monocytes, and $CD3^-/CD16^+$ NK-T lymphocytes. [^{3}H](R)-PK11195 B_{max} values *in vivo* correlated negatively with $CD3^+/CD4^+/CD29^+$ memory subsets of $CD4^+$ T lymphocytes, MAP-2, and SYN levels. None of the other cell types correlated with [^{3}H](R)-PK11195 B_{max} values. Correlations were performed using 95% confidence intervals. Results from nonparametric correlational analyses are represented by *r*, the Spearman's coefficient and *P* values below 0.05 were considered significant.

receptors per cell. We are currently unable to determine the exact numbers of brain macrophages versus astrocytes in any given sample of brain tissue because of technical limitations. However, previous studies have indicated that PK11195 binding in SIVE both in brain tissues[18,32] as well as *in vivo*[18] correlate closely with the abundance of brain macrophages but not the abundance of reactive astrocytes. These data taken together, support the overall hypothesis that PK11195 indeed labels infected and activated brain macrophages in lentiviral encephalitis.

Of seven SIV-infected macaques, five showed higher levels of [^{11}C](R)-PK11195 retention in the brain corre-

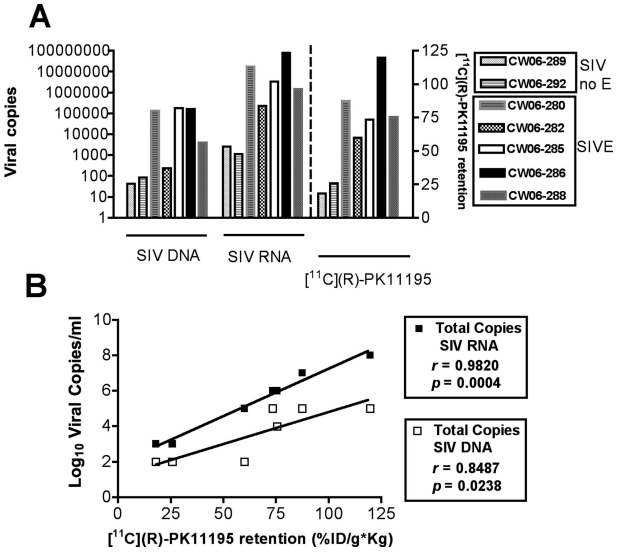

Figure 5. [^{11}C](R)-PK11195 retention *in vivo* correlates with postmortem brain viral loads. **A** and **B:** SIV RNA and DNA (**A**, viral copies, left *y* axis) were determined in postmortem frontal cortical tissue of macaques with SIVE and SIV infected without encephalitis (SIV no E) and were compared with premortem [^{11}C](R)-PK11195 retention (%ID/g*kg) in the frontal cortex in these same animals (**A**, right *y* axis). [^{11}C](R)-PK11195 retention (%ID/g*kg, *x* axis) was correlated with levels of both SIV RNA and DNA (**B**, Log_{10} viral copies).

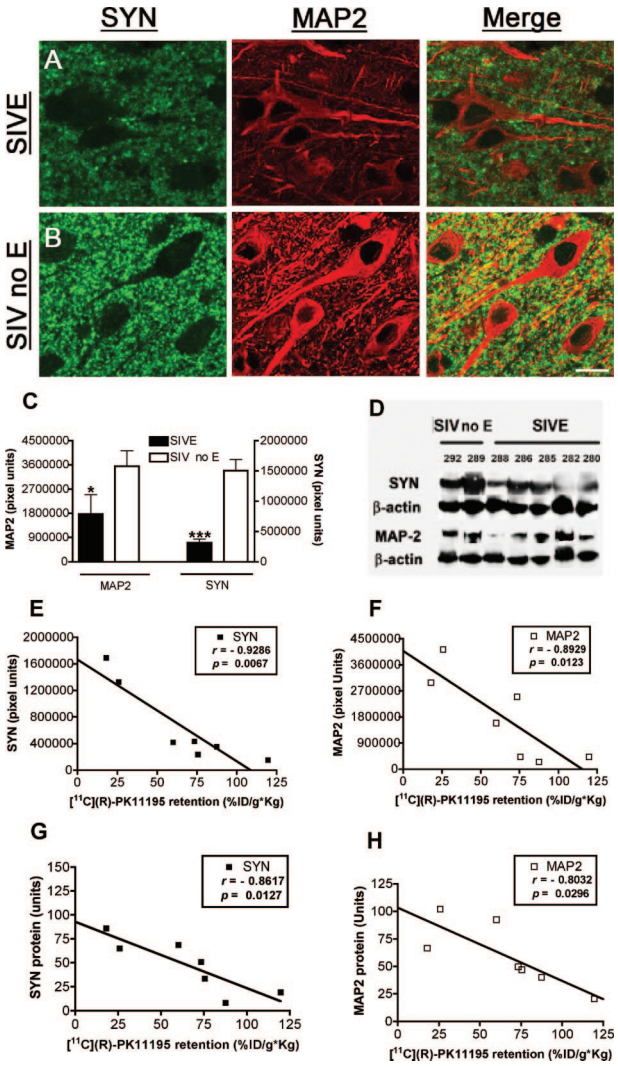

Figure 6. [^{11}C](R)-PK11195 retention *in vivo* correlates with areas of synaptic degeneration. **A–C:** Frontal cortical tissue obtained from macaques with SIVE (**A**) and SIV infected without encephalitis (SIV no E, **B**) were stained with the presynaptic protein synaptophysin (SYN, green) and the postsynaptic protein microtubule-associated protein-2 (MAP-2, red). **C:** MAP-2 (left *y* axis) and SYN (right *y* axis) immunofluorescence was quantified in SIVE macaques and compared to nonencephalitic macaques (SIV no E). Data were analyzed using Student's *t*-test, $^{***}P < 0.0001$, $^{*}P < 0.05$. **D:** Western blot analysis of MAP-2 and SYN in frontal cortical tissue obtained from macaques with SIVE and SIV infected without encephalitis (SIV no E) with β-actin as an internal control. **E** and **F:** SYN (**D**) and MAP-2 (**E**) quantified by immunofluorescence (*y* axis, pixel units) in frontal cortical tissue of macaques with SIVE and SIV infected without encephalitis (SIV no E) were correlated with premortem [^{11}C](R)-PK11195 retention (%ID/g*kg, *x* axis) in the frontal cortex in these same animals. **G** and **H:** SYN (**G**) and MAP-2 (**H**) quantified by Western blotting and normalized to β-actin levels (*y* axis, arbitrary units) in frontal cortical tissue of macaques with SIVE and SIV infected without encephalitis (SIV no E) were correlated with premortem [^{11}C](R)-PK11195 retention (%ID/g*kg, *x* axis) in the frontal cortex in these same animals.

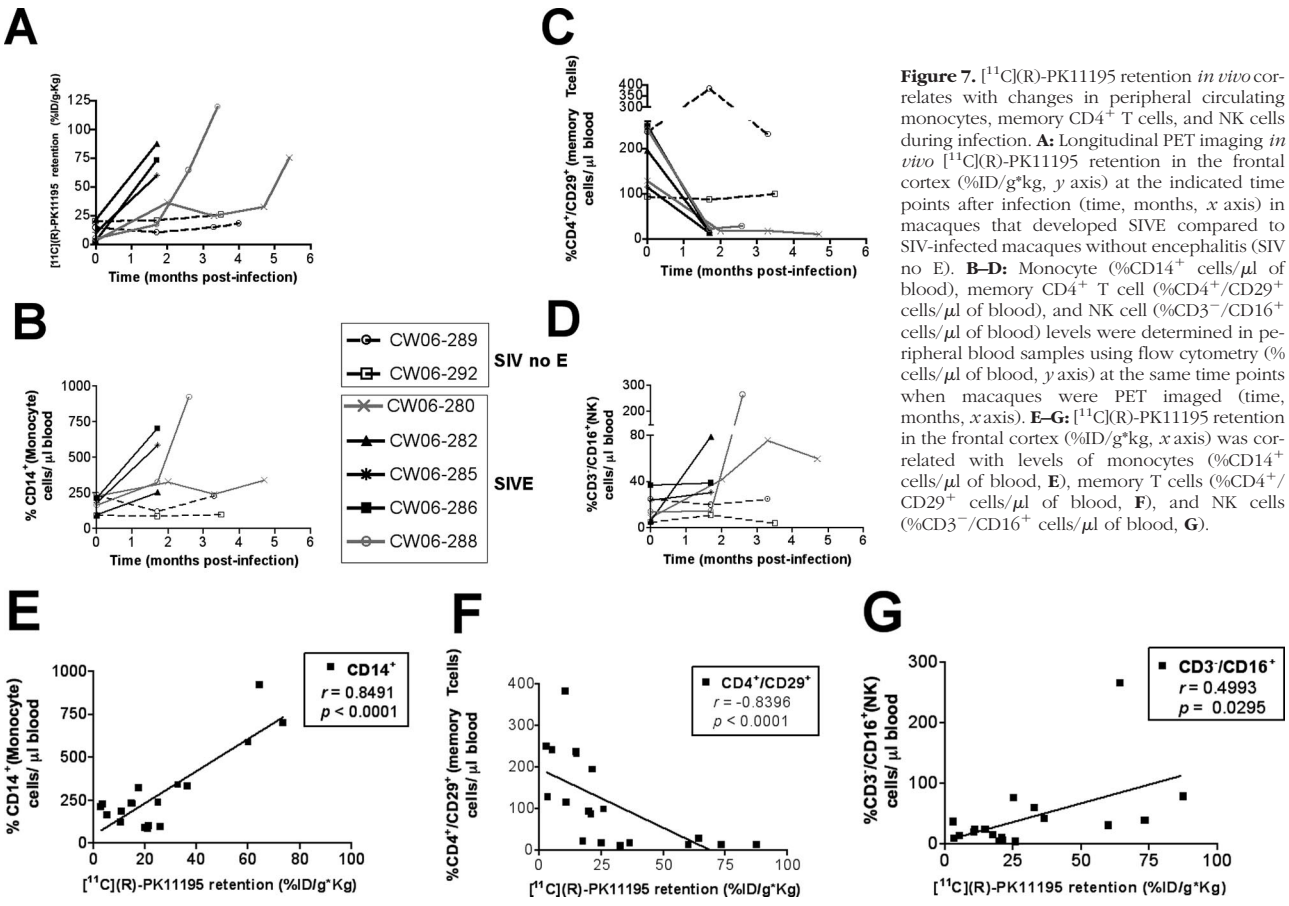

Figure 7. [^{11}C](R)-PK11195 retention *in vivo* correlates with changes in peripheral circulating monocytes, memory CD4$^+$ T cells, and NK cells during infection. **A:** Longitudinal PET imaging *in vivo* [^{11}C](R)-PK11195 retention in the frontal cortex (%ID/g*kg, *y* axis) at the indicated time points after infection (time, months, *x* axis) in macaques that developed SIVE compared to SIV-infected macaques without encephalitis (SIV no E). **B–D:** Monocyte (%CD14$^+$ cells/μl of blood), memory CD4$^+$ T cell (%CD4$^+$/CD29$^+$ cells/μl of blood), and NK cell (%CD3$^-$/CD16$^+$ cells/μl of blood) levels were determined in peripheral blood samples using flow cytometry (% cells/μl of blood, *y* axis) at the same time points when macaques were PET imaged (time, months, *x* axis). **E–G:** [^{11}C](R)-PK11195 retention in the frontal cortex (%ID/g*kg, *x* axis) was correlated with levels of monocytes (%CD14$^+$ cells/μl of blood, **E**), memory T cells (%CD4$^+$/CD29$^+$ cells/μl of blood, **F**), and NK cells (%CD3$^-$/CD16$^+$ cells/μl of blood, **G**).

sponding to the presence of SIVE on postmortem examination. Two macaques that did not show an increase in [^{11}C](R)-PK11195 retention in the brain did not develop SIVE (Figure 3). Increased [^{11}C](R)-PK11195 retention in encephalitic macaques was observed in all brain regions assessed, consistent with the multifocality of disease without a prominent neuroanatomical distribution[27] similar to human postmortem studies implicating several brain regions including the basal ganglia, frontal cortex, and hippocampus (Figure 3).[37,38] Three of the five encephalitic macaques rapidly progressed to AIDS in less than 2 months (Table 2). Interestingly, macaque CW06-280 the longest lived in its cohort (174 days) showed increases in [^{11}C](R)-PK11195 retention and sustained high CSF viral loads ~4 months after infection (Figures 3 and 4). Histopathologically, this macaque showed abundant brain infiltration with activated macrophage and microglial nodules, but fewer numbers of cells staining for SIV. SIV DNA and RNA levels in this macaque were intermediate between the encephalitic and nonencephalitic macaques. It is possible that this macaque represents an early form of SIVE. Viral loads in CSF, but not in plasma correlated significantly with *in vivo* [^{11}C](R)-PK11195 retention in all brain regions assessed (Figure 3 and Table 3). These data agree with reports that suggest that CSF viral loads are higher in macaques that develop encephalitis[39] and correlate with the degree of cognitive impairment and encephalitis in HIVD.[40,41]

Although the sample size in this study is small, we have previously shown that [^{11}C](R)-PK11195 is able to detect activated brain macrophages *in vivo* in a cohort of terminal encephalitic macaques.[18] These studies taken together with previous reports that use [^{11}C](R)-PK11195 to label activated brain macrophages *in vivo*,[17] support the use of [^{11}C](R)-PK11195 as a diagnostic tool to detect HIV encephalitis. However, [^{11}C](R)-PK11195 imaging studies in human patients have been less promising with no differences between HIV-infected individuals with or without mild neurological deficits.[42,43] It has been suggested that anti-retroviral therapy in HIV-infected patients decreases the incidence and severity of neurological disease.[15] Indeed the clinical neurological symptoms of these patients are reported to be less severe than frank dementia and are termed minor cognitive motor disorder.[44] Further, the neuropathology seen in these patients is also different from frank encephalitis with subtle degeneration of dendritic arbors and interneuron populations,[45] with very low to undetectable CSF HIV viral RNA.[46] None of the patients in both these studies had frank dementia suggesting that [^{11}C](R)-PK11195 may lack the sensitivity to detect subtle to milder forms of disease. Interestingly, the prevalence of HIVD has been suggested to be increasing because of longer lifespans of HIV-infected patients with better peripheral control of viremia.[47,48] Future studies in patients with and without HIVD will determine whether [^{11}C](R)-PK1119 can be

used to detect and monitor more chronic forms of disease in patients on anti-retroviral therapy. Future studies in SIV-infected macaques with and without anti-retroviral therapy will determine whether [^{11}C](R)-PK11195 is able to detect development and progression of disease during therapies.

Synaptic degeneration has been reported in lentiviral encephalitis and is hypothesized to be the basis for neurological deficits seen in HIVD.[49] Increases in [^{11}C](R)-PK11195 retention *in vivo* correlated with decreases in both SYN and MAP-2 suggesting that [^{11}C](R)-PK11195 retention corresponded to areas with synaptic degeneration. Because markers for activated and infected macrophages correlate with synaptic damage,[27,31] these data further support the hypothesis that PK11195 labels infected and activated macrophages.

Our results indicate that CD14$^+$ monocyte levels in the peripheral blood, but not total numbers of PBMCs correlate significantly with *in vivo* [^{11}C](R)-PK11195 retention during infection (Figure 7, A and B). Because PK11195 labels activated and infected macrophages, it is possible that *in vivo* [^{11}C](R)-PK11195 retention may represent a measure of monocytes trafficking into the CNS. We assessed changes in several peripheral factors that influence viral control in parallel with longitudinal PET imaging with [^{11}C](R)-PK11195. *In vivo* [^{11}C](R)-PK11195 retention did not correlate with declines in total numbers of CD4$^+$ or CD8$^+$ T lymphocytes, consistent with previous studies.[13] However, decline in CD4$^+$/CD29$^+$ subsets of CD4$^+$ T cells correlated with *in vivo* [^{11}C](R)-PK11195 retention in all brain regions assessed (Figure 7 and Table 3). CD29, along with CD49, is part of a heterodimer forming the integrin VLA-4 that binds to vascular cell adhesion molecule-1, which is expressed on activated endothelial cells. The CD29$^+$/CD45RO$^+$ memory subset of CD4$^+$ T cells responds to stimulation by recall antigens and provides B-cell help for immunoglobulin production.[50] In humans, these memory CD4$^+$ T cells are preferentially infected with HIV and are thought to represent the principal reservoir for virus within CD4$^+$ T cells.[51] *In vivo* [^{11}C](R)-PK11195 correlation with a decline in this subset of memory CD4$^+$ T cells may represent a marker for rapid progression of disease and the development of encephalitis.

The role of NK cells in HIV infection and their cytolytic and noncytolytic response to infected cells has been extensively studied.[52] During acute infection a subset of NK cells that are defective in cytolytic function expressing CD3$^-$/CD56$^-$/CD16$^+$ undergo expansion.[52,53] We observed a longitudinal correlation between increased numbers of CD3$^-$/CD16$^+$ and *in vivo* [^{11}C](R)-PK11195 retention (Figure 7 and Table 3). Although we did not analyze CD56 expression and cytolytic function in this cell group, it is possible that increases in this population of dysfunctional NK cells is a correlate of rapid progression and the development of encephalitis. This observation is supported by a previous study suggesting that NK cell activity is dysfunctional in macaques that eventually develop encephalitis compared to macaques that do not.[54] Finally, we assessed changes in platelet numbers in parallel with *in vivo* [^{11}C](R)-PK11195 retention. It has been suggested that high decline in platelet numbers is a predictive feature of SIVE.[55] We were unable to detect any significant correlation between platelet numbers and *in vivo* [^{11}C](R)-PK11195 retention in our macaque cohort.

Our studies show that longitudinal [^{11}C](R)-PK11195 PET imaging of SIV-infected macaques is able to label infected and activated macrophages in the brain *in vivo* corresponding to the development of encephalitis. Increases in [^{11}C](R)-PK11195 retention in the brain correlated with increased CSF viral loads. Moreover, [^{11}C](R)-PK11195 retention in the brain correlated with increases in circulating peripheral monocyte levels suggesting that PK11195 might represent a surrogate measure of CNS-infiltrating monocytes that differentiate to form macrophages. Finally [^{11}C](R)-PK11195 retention correlated with increases in presumably dysfunctional NK cell numbers and with decreases in CD4$^+$ memory T cells. These latter might represent peripheral correlates of rapid disease progression and the development of encephalitis. Our results suggest that a combination of PET imaging with [^{11}C](R)-PK11195 and assessment of the described peripheral immune parameters might help in the clinical detection and therapeutic monitoring of HIVD.

Acknowledgments

We thank Jonette Werley, James Kasenchak, Aaron Schmookler, John Saunders, Jason Nugyen, and Adam Starkey for valuable technical assistance; Premeela Rajakumaran for CSF and plasma viral RNA analyses; Heather Michaels for flow cytometric analyses; Susan Slagel and James Ruszkiewicz for help with the PET scans; and Dawn L. Clements-McBride for assistance in obtaining information about the macaques.

References

1. McArthur JC: NeuroAIDS: diagnosis and management. Hosp Pract 1997, 32:73–84
2. Dore GJ, Correll PK, Li Y, Kaldor JM, Cooper DA, Brew BJ: Changes to AIDS dementia complex in the era of highly active antiretroviral therapy. AIDS 1999, 13:1249–1253
3. Brew BJ: AIDS dementia complex. Neurol Clin 1999, 17:861–881
4. Baskin GB, Murphey-Corb M, Roberts ED, Didier PJ, Martin LN: Correlates of SIV encephalitis in rhesus monkeys. J Med Primatol 1992, 21:59–63
5. Budka H: Neuropathology of human immunodeficiency virus infection. Brain Pathol 1991, 1:163–175
6. Lackner AA, Smith MO, Munn RJ, Martfeld DJ, Gardner MB, Marx PA, Dandekar S: Localization of simian immunodeficiency virus in the central nervous system of rhesus monkeys. Am J Pathol 1991, 139:609–621
7. Wang TH, Donaldson YK, Brettle RP, Bell JE, Simmonds P: Identification of shared populations of human immunodeficiency virus type 1 infecting microglia and tissue macrophages outside the central nervous system. J Virol 2001, 75:11686–11699
8. Mankowski JL, Flaherty MT, Spelman JP, Hauer DA, Didier PJ, Amedee AM, Murphey-Corb M, Kirstein LM, Munoz A, Clements JE, Zink MC: Pathogenesis of simian immunodeficiency virus encephalitis: viral determinants of neurovirulence. J Virol 1997, 71:6055–6060
9. Reddy RT, Achim CL, Sirko DA, Tehranchi S, Kraus FG, Wong-Staal F, Wiley CA: Sequence analysis of the V3 loop in brain and spleen of patients with HIV encephalitis. AIDS Res Hum Retroviruses 1996, 12:477–482

10. Gorry PR, Bristol G, Zack JA, Ritola K, Swanstrom R, Birch CJ, Bell JE, Bannert N, Crawford K, Wang H, Schols D, De Clercq E, Kunstman K, Wolinsky SM, Gabuzda D: Macrophage tropism of human immunodeficiency virus type 1 isolates from brain and lymphoid tissues predicts neurotropism independent of coreceptor specificity. J Virol 2001, 75:10073–10089
11. Bouwman FH, Skolasky RL, Hes D, Selnes OA, Glass JD, Nance-Sproson TE, Royal W, Dal Pan GJ, McArthur JC: Variable progression of HIV-associated dementia. Neurology 1998, 50:1814–1820
12. Adamson DC, McArthur JC, Dawson TM, Dawson VL: Rate and severity of HIV-associated dementia (HAD): correlations with Gp41 and iNOS. Mol Med 1999, 5:98–109
13. Westmoreland SV, Halpern E, Lackner AA: Simian immunodeficiency virus encephalitis in rhesus macaques is associated with rapid disease progression. J Neurovirol 1998, 4:260–268
14. O'Neil SP, Suwyn C, Anderson DC, Niedziela G, Bradley J, Novembre FJ, Herndon JG, McClure HM: Correlation of acute humoral response with brain virus burden and survival time in pig-tailed macaques infected with the neurovirulent simian immunodeficiency virus SIVsmmFGb. Am J Pathol 2004, 164:1157–1172
15. Gray F, Chretien F, Vallat-Decouvelaere AV, Scaravilli F: The changing pattern of HIV neuropathology in the HAART era. J Neuropathol Exp Neurol 2003, 62:429–440
16. Cysique LA, Maruff P, Brew BJ: Variable benefit in neuropsychological function in HIV-infected HAART-treated patients. Neurology 2006, 66:1447–1450
17. Banati RB: Visualising microglial activation in vivo. Glia 2002, 40:206–217
18. Venneti S, Lopresti BJ, Wang G, Bissel SJ, Mathis CA, Meltzer CC, Boada F, Capuano S III, Kress GJ, Davis DK, Ruszkiewicz J, Reynolds IJ, Murphey-Corb M, Trichel AM, Wisniewski SR, Wiley CA: PET imaging of brain macrophages using the peripheral benzodiazepine receptor in a macaque model of neuroAIDS. J Clin Invest 2004, 113:981–989
19. Bissel SJ, Wang G, Trichel AM, Murphey-Corb M, Wiley CA: Longitudinal analysis of monocyte/macrophage infection in simian immunodeficiency virus-infected $CD8^+$ T-cell-depleted macaques that develop lentiviral encephalitis. Am J Pathol 2006, 168:1553–1569
20. Bergamini A, Faggioli E, Bolacchi F, Gessani S, Cappannoli L, Uccella I, Demin F, Capozzi M, Cicconi R, Placido R, Vendetti S, Colizzi GM, Rocchi G: Enhanced production of tumor necrosis factor-alpha and interleukin-6 due to prolonged response to lipopolysaccharide in human macrophages infected in vitro with human immunodeficiency virus type 1. J Infect Dis 1999, 179:832–842
21. Barami K, Grever WE, Diaz FG, Lyman WD: An efficient method for the culturing and generation of neurons and astrocytes from second trimester human central nervous system tissue. Neurol Res 2001, 23:321–326
22. Padmanabhan J, Clayton D, Shelanski ML: Dibutyryl cyclic AMP-induced process formation in astrocytes is associated with a decrease in tyrosine phosphorylation of focal adhesion kinase and paxillin. J Neurobiol 1999, 39:407–422
23. Shah F, Hume SP, Pike VW, Ashworth S, McDermott J: Synthesis of the enantiomers of [N-methyl-11C]PK 11195 and comparison of their behaviours as radioligands for PK binding sites in rats. Nucl Med Biol 1994, 21:573–581
24. Woods RP, Cherry SR, Mazziotta JC: Rapid automated algorithm for aligning and reslicing PET images. J Comput Assist Tomogr 1992, 16:620–633
25. Cline AN, Bess JW, Piatak M Jr, Lifson JD: Highly sensitive SIV plasma viral load assay: practical considerations, realistic performance expectations, and application to reverse engineering of vaccines for AIDS. J Med Primatol 2005, 34:303–312
26. Mummidi S, Bamshad M, Ahuja SS, Gonzalez E, Feuillet PM, Begum K, Galvis MC, Kostecki V, Valente AJ, Murthy KK, Haro L, Dolan MJ, Allan JS, Ahuja SK: Evolution of human and non-human primate CC chemokine receptor 5 gene and mRNA. Potential roles for haplotype and mRNA diversity, differential haplotype-specific transcriptional activity, and altered transcription factor binding to polymorphic nucleotides in the pathogenesis of HIV-1 and simian immunodeficiency virus. J Biol Chem 2000, 275:18946–18961
27. Bissel SJ, Wang G, Ghosh M, Reinhart TA, Capuano S III, Stefano Cole K, Murphey-Corb M, Piatak M Jr, Lifson JD, Wiley CA: Macrophages relate presynaptic and postsynaptic damage in simian immunodeficiency virus encephalitis. Am J Pathol 2002, 160:927–941
28. Seman AL, Pewen WF, Fresh LF, Martin LN, Murphey-Corb M: The replicative capacity of rhesus macaque peripheral blood mononuclear cells for simian immunodeficiency virus in vitro is predictive of the rate of progression to AIDS in vivo. J Gen Virol 2000, 81: 2441–2449
29. Bissel SJ, Wang G, Trichel AM, Murphey-Corb M, Wiley CA: Longitudinal analysis of activation markers on monocyte subsets during the development of simian immunodeficiency virus encephalitis. J Neuroimmunol 2006, 177:85–98
30. Banati RB, Newcombe J, Gunn RN, Cagnin A, Turkheimer F, Heppner F, Price G, Wegner F, Giovannoni G, Miller DH, Perkin GD, Smith T, Hewson AK, Bydder G, Kreutzberg GW, Jones T, Cuzner ML, Myers R: The peripheral benzodiazepine binding site in the brain in multiple sclerosis: quantitative in vivo imaging of microglia as a measure of disease activity. Brain 2000, 123:2321–2337
31. Masliah E, Achim CL, Ge N, DeTeresa R, Terry RD, Wiley CA: Spectrum of human immunodeficiency virus-associated neocortical damage. Ann Neurol 1992, 32:321–329
32. Mankowski JL, Queen SE, Tarwater PJ, Adams RJ, Guilarte TR: Elevated peripheral benzodiazepine receptor expression in simian immunodeficiency virus encephalitis. J Neurovirol 2003, 9:94–100
33. McEnery MW, Snowman AM, Trifiletti RR, Snyder SH: Isolation of the mitochondrial benzodiazepine receptor: association with the voltage-dependent anion channel and the adenine nucleotide carrier. Proc Natl Acad Sci USA 1992, 89:3170–3174
34. Everett H, Barry M, Sun X, Lee SF, Frantz C, Berthiaume LG, McFadden G, Bleackley RC: The myxoma poxvirus protein. M11L, prevents apoptosis by direct interaction with the mitochondrial permeability transition pore. J Exp Med 2002, 196:1127–1139
35. Johnston C, Jiang W, Chu T, Levine B: Identification of genes involved in the host response to neurovirulent alphavirus infection. J Virol 2001, 75:10431–10445
36. Aquaro S, Bagnarelli P, Guenci T, De Luca A, Clementi M, Balestra E, Calio R, Perno CF: Long-term survival and virus production in human primary macrophages infected by human immunodeficiency virus. J Med Virol 2002, 68:479–488
37. Brew BJ, Rosenblum M, Cronin K, Price RW: AIDS dementia complex and HIV-1 brain infection: clinical-virological correlations. Ann Neurol 1995, 38:563–570
38. Moore DJ, Masliah E, Rippeth JD, Gonzalez R, Carey CL, Cherner M, Ellis RJ, Achim CL, Marcotte TD, Heaton RK, Grant I: Cortical and subcortical neurodegeneration is associated with HIV neurocognitive impairment. AIDS 2006, 20:879–887
39. Zink MC, Suryanarayana K, Mankowski JL, Shen A, Piatak M Jr, Spelman JP, Carter DL, Adams RJ, Lifson JD, Clements JE: High viral load in the cerebrospinal fluid and brain correlates with severity of simian immunodeficiency virus encephalitis. J Virol 1999, 73:10480-10488
40. McArthur JC, McClernon DR, Cronin MF, Nance-Sproson TE, Saah AJ, St Clair M, Lanier ER: Relationship between human immunodeficiency virus-associated dementia and viral load in cerebrospinal fluid and brain. Ann Neurol 1997, 42:689–698
41. Cinque P, Vago L, Ceresa D, Mainini F, Terreni MR, Vagani A, Torri W, Bossolasco S, Lazzarin A: Cerebrospinal fluid HIV-1 RNA levels: correlation with HIV encephalitis. AIDS 1998, 12:389–394
42. Hammoud DA, Endres CJ, Chander AR, Guilarte TR, Wong DF, Sacktor NC, McArthur JC, Pomper MG: Imaging glial cell activation with [11C]-R-PK11195 in patients with AIDS. J Neurovirol 2005, 11:346–355
43. Wiley CA, Lopresti BJ, Becker JT, Boada F, Lopez OL, Mellors J, Meltzer CC, Wisniewski SR, Mathis CA: Positron emission tomography imaging of peripheral benzodiazepine receptor binding in human immunodeficiency virus-infected subjects with and without cognitive impairment. J Neurovirol 2006, 12:262–271
44. Clinical confirmation of the American Academy of Neurology algorithm for HIV-1-associated cognitive/motor disorder. The Dana Consortium on Therapy for HIV Dementia and Related Cognitive Disorders. Neurology 1996, 47:1247–1253
45. Langford TD, Letendre SL, Larrea GJ, Masliah E: Changing patterns in the neuropathogenesis of HIV during the HAART era. Brain Pathol 2003, 13:195–210
46. McArthur JC, McDermott MP, McClernon D, St Hillaire C, Conant K,

Marder K, Schifitto G, Selnes OA, Sacktor N, Stern Y, Albert SM, Kieburtz K, deMarcaida JA, Cohen B, Epstein LG: Attenuated central nervous system infection in advanced HIV/AIDS with combination antiretroviral therapy. Arch Neurol 2004, 61:1687–1696
47. Valcour VG, Shikuma CM, Watters MR, Sacktor NC: Cognitive impairment in older HIV-1-seropositive individuals: prevalence and potential mechanisms. AIDS 2004, 18(Suppl 1):S79–S86
48. Geraci AP, Simpson DM: Neurological manifestations of HIV-1 infection in the HAART era. Compr Ther 2001, 27:232–241
49. Ellis R, Langford D, Masliah E: HIV and antiretroviral therapy in the brain: neuronal injury and repair. Nat Rev Neurosci 2007, 8:33–44
50. Damle NK, Doyle LV: Ability of human T lymphocytes to adhere to vascular endothelial cells and to augment endothelial permeability to macromolecules is linked to their state of post-thymic maturation. J Immunol 1990, 144:1233–1240
51. Schnittman SM, Lane HC, Greenhouse J, Justement JS, Baseler M, Fauci AS: Preferential infection of $CD4^+$ memory T cells by human immunodeficiency virus type 1: evidence for a role in the selective T-cell functional defects observed in infected individuals. Proc Natl Acad Sci USA 1990, 87:6058–6062
52. Fauci AS, Mavilio D, Kottilil S: NK cells in HIV infection: paradigm for protection or targets for ambush. Nat Rev Immunol 2005, 5:835–843
53. Mavilio D, Lombardo G, Benjamin J, Kim D, Follman D, Marcenaro E, O'Shea MA, Kinter A, Kovacs C, Moretta A, Fauci AS: Characterization of CD56−/CD16+ natural killer (NK) cells: a highly dysfunctional NK subset expanded in HIV-infected viremic individuals. Proc Natl Acad Sci USA 2005, 102:2886–2891
54. Shieh TM, Carter DL, Blosser RL, Mankowski JL, Zink MC, Clements JE: Functional analyses of natural killer cells in macaques infected with neurovirulent simian immunodeficiency virus. J Neurovirol 2001, 7:11–24
55. Wachtman LM, Tarwater PM, Queen SE, Adams RJ, Mankowski JL: Platelet decline: an early predictive hematological marker of simian immunodeficiency virus central nervous system disease. J Neurovirol 2006, 12:25–33